

---

---

# Bilateral Hilar Foci on $^{18}\text{F}$ -FDG PET Scan in Patients Without Lung Cancer: Variables Associated with Benign and Malignant Etiology

Maroun Karam<sup>1</sup>, Shayna Roberts-Klein<sup>1</sup>, Narendra Shet<sup>2</sup>, Johanna Chang<sup>2</sup>, and Paul Feustel<sup>3</sup>

<sup>1</sup>Nuclear Medicine Section, Radiology Department, Albany Medical College, Albany, New York; <sup>2</sup>Neuropharmacology, Radiology Department, Albany Medical College, Albany, New York; and <sup>3</sup>Neurosciences & Biostatistics, Radiology Department, Albany Medical College, Albany, New York

Bilateral hilar  $^{18}\text{F}$ -FDG-avid foci are often noted on PET studies of patients without lung cancer. This finding may lead to diagnostic uncertainty about the presence of metastatic disease. Our objective was to evaluate features of these foci associated with benign or malignant etiology. **Methods:** We performed a retrospective study of patients with cancer with bilateral hilar foci on 1 or 2 sequential  $^{18}\text{F}$ -FDG PET studies between 2002 and 2006. Patients with lung cancer, sarcoidosis, or anthracosis/silicosis were excluded. Variables evaluated were maximum standard uptake values (SUV max), purity (absence of  $^{18}\text{F}$ -FDG-avid foci in nonhilar mediastinal nodes), symmetry (difference between left and right side SUV max), the primary tumor, node size determined by CT, and, in those who participated in 2 studies, stability of uptake over time. The gold standard was histologic diagnosis or long-term clinical follow-up (range, 19–41 mo; mean, 25 mo). **Results:** Fifty-one patients with the finding of bilateral hilar  $^{18}\text{F}$ -FDG-avid foci underwent a staging-only PET study; 52 scans from an additional set of patients demonstrated this abnormality on at least 1 of 2 sequential studies, the first of which was performed for staging. On univariate analysis, variables associated with malignancy were SUV max ( $6.6 \pm 4.1$  vs.  $3.5 \pm 1.0$  for benign,  $P < 0.001$ ;  $t$  test); impurity ( $P < 0.001$ ;  $\chi^2$  test), with 79% of impure scans versus 18% of pure scans being malignant; node size determined by CT ( $P = 0.027$ ); and change in uptake between scans 1 and 2 (change in SUV =  $2.7 \pm 2.1$  vs.  $0.73 \pm 1.1$  for benign,  $P < 0.01$ ;  $t$  test). Variables associated with benign etiology were: symmetry (difference between left and right sides =  $0.57 \pm 0.54$  for benign vs.  $1.8 \pm 1.7$  for malignant,  $P < 0.01$ ), purity, and colorectal primary (75% of colorectal were benign vs. 34% of breast, 49% of lymphoma, and 37% of other,  $P = 0.030$ ;  $\chi^2$  test). After multivariate analysis, SUV max and purity were found to be independent predictors, with the odds of malignancy increasing by 1.54 (95% confidence interval, 1.16–2.05) for each unit increase in SUV and decreasing by 0.08 (95% confidence interval, 0.03–0.22) if pure. **Conclusion:** In patients with nonlung cancer, in particular colorectal, foci of symmetric and mild uptake limited to the hilar regions that are stable on 2 sequential PET stud-

ies despite intervening anticancer therapy are likely related to a benign etiology.

**Key Words:**  $^{18}\text{F}$ -FDG PET scan; bilateral hilar foci; benign

**J Nucl Med 2008; 49:1429–1436**

DOI: 10.2967/jnumed.107.048983

---

**B**ilateral hilar  $^{18}\text{F}$ -FDG-avid foci are often noted on PET studies of patients with cancer outside the lungs. The clinical significance of these foci can be unclear and may lead to diagnostic uncertainty about the presence of metastatic disease. If the interpreting physician suggests metastatic disease, but the finding turns out to be false-positive, this misinterpretation may lead to unnecessary treatment of the patient with toxic drugs. If, on the other hand, the finding is dismissed as benign but a malignancy is involved, undertreatment of a potentially fatal condition would have occurred. Pathologic evaluation is not easy because sampling of the hilar nodes is not part of standard mediastinoscopy (1). Obtaining tissue from the hilar nodes requires a targeted approach either with a CT-guided biopsy or preferably with the help of endobronchial ultrasound (2,3). If adequate tissue is not collected by 1 of these 2 methods, video-assisted thoracoscopic surgery, an invasive approach requiring a hospital stay, can be used (4). Video-assisted thoracoscopic surgery is not without danger, because vascular structures are present in the hilum. The most common solution to this diagnostic dilemma used by interpreting physicians is to recommend short-term follow-up. This approach delays treatment if the tumor is malignant, but the patient may experience unnecessary anxiety if the tumor is benign. If the findings remain unchanged on the next PET/CT scan, they are often considered benign. However, no data in the literature exist, to our knowledge, to prove or disprove this assertion.

Actually, to our knowledge, there has not been any systematic attempt yet to evaluate the often puzzling finding of  $^{18}\text{F}$ -FDG-avid hilar foci and to correlate its characteristics with ultimate outcome. Some of the features

---

Received Nov. 13, 2007; revision accepted May 28, 2008.  
For correspondence or reprints contact: Maroun Karam, Albany Medical College, 43 New Scotland Ave., MC-113 Albany, NY 12208.  
E-mail: karamm@mail.amc.edu  
COPYRIGHT © 2008 by the Society of Nuclear Medicine, Inc.

of hilar foci that could potentially be studied include the intensity of uptake, symmetry (difference in SUV between uptake on the left and the right), presence or absence of other  $^{18}\text{F}$ -FDG-avid nodes in the mediastinum, stability or lack thereof of uptake on sequential studies, nature of the primary cancer, and dimensions or appearance on CT study. Our objective was to evaluate the features of these foci associated with a benign or malignant etiology. Specifically we wanted to answer the following question: In patients with cancer outside the lungs and bilateral hilar foci, is there a benign pattern that would not require a biopsy or a repeated PET/CT scan in a few months? Such a pattern would be reassuring to the referring physician and the patient and would save unnecessary expense and anxiety.

## MATERIALS AND METHODS

### Patient Selection

We performed a retrospective analysis of patients with cancer with bilateral hilar foci on 1 or 2 sequential  $^{18}\text{F}$ -FDG PET studies between 2002 and 2006. In February 2006, our PET unit was upgraded to a PET/CT scanner by adding a 4-slice CT scanner to the PET system. The PET acquisition protocol remained the same during the entire study period.

Patients had a variety of malignancies, with breast, colorectal, and lymphoma being the most common. Patients with lung cancer were excluded. During the period outlined, we performed 366 initial-staging scans only on patients with nonlung cancer and identified 51 patients with bilateral hilar foci (or an incidence of 13.9%). Similarly, we performed at least 2 sequential PET scans on an additional 627 patients with cancer outside the lung and found 52 patients with bilateral hilar foci (8.2%). As described above, 103 patients fulfilled the eligibility criteria. Fifty-one patients (25 women and 26 men; age range, 26–94 y) had only 1 PET scan (all initial-staging studies; group I), and 52 patients (19 women and 33 men; age range, 20–97 y) had at least 2 sequential PET scans, the first one performed for initial staging (group II). Of the 51 group I patients, 30 underwent PET alone and 21 underwent PET/CT. In group II, 28 patients had both scans by PET alone, 14 had both scans by PET/CT, and 10 had the first scan with PET and the second scan with PET/CT. Of the 103 patients, 53 were diagnosed with malignant disease (31 in group I and 22 in group II) and 50 (20 in group I and 30 in group II) with a benign etiology.

### Scan Acquisition

Each patient underwent intravenous injection of 592–703 MBq of  $^{18}\text{F}$ -FDG. Approximately 60 min after injection, patients were scanned from the base of the brain to the proximal thigh area. Attenuation-corrected and non-attenuation-corrected images were obtained by a dedicated PET scanner (Advance NXI; GE Healthcare). Emission scanning was performed with a weight-based protocol, with 4–6 min per bed position, and transmission scanning was performed with 2 min per bed position. Emission images were reconstructed by using an iterative algorithm with 16 subsets, using segmented attenuation correction. The matrix size was  $128 \times 128$ , and the field of view was 55 cm. Transmission reconstruction parameters consisted of images being reconstructed using segmented attenuation correction.

### Image Quantification

Image interpretation was performed on a workstation (AW42P; GE Healthcare) using coronal, sagittal, and transaxial planes and 3-dimensional projections. Semiquantitative analysis of images was performed by measuring the maximum standardized uptake values (SUV max) of bilateral hilar foci. The slice used for the SUV measurement was selected on the basis of visual analysis. More specifically, in volume viewer mode on the GE workstation, SUVs were derived from pixels in the PET raw data. A volume of interest deposited on a slice will automatically calculate the SUV max of the pixel with the highest uptake of  $^{18}\text{F}$ -FDG in that area. The size of the volume of interest can be adjusted to include only the area to be measured. SUV max was measured in this manner for each hilar focus and recorded for each patient.

### Data Analysis

Categorical variables that were tested included primary malignancy in 4 categories (breast, colorectal, lymphoma, and other); purity of the scan, defined as absence of  $^{18}\text{F}$ -FDG-avid foci in other nonhilar mediastinal nodes; and a subjective assessment of node size by CT (enlarged or not) in patients who had their entire evaluation done by PET/CT ( $n = 35$ ). Quantitative assessment of node size by CT could not be done because of the difficulty in delineating the nodal contours and distinguishing the node from adjacent blood vessels on a CT image obtained without contrast material and with a low dose. Continuous variables investigated included intensity of uptake measured by SUV max, including in the case of group II patients the SUV max of the first scan; symmetry measured by absolute and relative change in SUV between the left and right side; and in the subset of patients with more than 1 scan, stability of uptake over time measured by the absolute and relative change in SUV between the first and the second scans. The gold standard for presence or absence of metastatic disease was histopathologic diagnosis (30 patients, 14 malignant and 16 benign) or long-term follow-up (range, 19–41 mo; mean, 25 mo; 73 patients, 39 malignant and 34 benign). Long-term follow-up was obtained by calling the referring physician and ascertaining the presence or absence of metastatic disease as established independently from the PET findings by clinical observation or other imaging modalities.

### Statistical Analysis

The association between malignancy and categorical variables was tested by  $\chi^2$  analysis. Differences in continuous variables between the malignant and benign groups were assessed by  $t$  tests. Stepwise multivariate logistic regression was performed to determine whether variables in combination could better predict malignancy. Candidate variables for the multivariate analysis were SUV max, symmetry expressed as percentage difference between left and right SUV max, purity, and primary tumor. Variables studied in univariate analysis included all the above plus difference in SUV between left and right, size by CT, and difference in SUV between scan 1 and scan 2 for patients in group II. Significance was accepted at the  $P < 0.05$  level. Analysis was performed using STATISTICA software (StatSoft).

Two control groups with bilateral  $^{18}\text{F}$ -FDG-avid hilar foci were analyzed separately; the first comprised 11 patients with biopsy-proven benign pulmonary nodules (group III). The second was a control group of 10 patients with cancer and granulomatous disease (sarcoidosis,  $n = 5$ ; anthracosis/silicosis,  $n = 4$ ; or asbestosis,  $n = 1$ ) (group IV). Size by CT variable was not

evaluated in the 2 control groups because none of these patients underwent PET/CT. Hilar nodes were not sampled in group III because the benign character of the nodules as proven by tissue diagnosis prevented further evaluation. For group IV, biopsy of the nodes was performed in 6 of 10 patients. For the remaining 4 patients, a history of granulomatous disease was documented by previous tissue diagnosis in 3, and occupational exposure to asbestos with calcified pleural plaques on CT was documented in 1.

## RESULTS

Data about the features of hilar foci in the 4 groups are described in Table 1.

The features of the hilar foci with benign pulmonary nodules (group III) are similar to those in patients with cancer and no metastatic disease. This finding suggests that the mechanism of hilar  $^{18}\text{F}$ -FDG uptake is not related to the presence of cancer. Because we proposed to answer a practical question about the presence or absence of metastatic disease in patients with cancer, this group was excluded from subsequent statistical analysis. Conversely, the hilar foci characteristics in patients with nonlung cancer and granulomatous disease are similar to those in patients with metastatic disease. In a patient with an unknown history of sarcoidosis, this finding would result in a false-positive PET impression for metastatic disease. However, for most patients in the latter group (8/10) a history of exposure (asbestos, sandblasting occupation) or sarcoidosis was known before the PET study was performed. In addition, certain suggestive signs (calcified pleural plaques and calcified lymph nodes) were seen on CT. In only 2 of 10 patients, a false impression of metastatic disease was suggested by the PET scan, but it was promptly corrected by a subsequent biopsy. Because our primary objective was not to identify benign disease but to identify a benign pattern, and because the features of hilar foci in group IV were similar to the features of those with metastatic disease, their inclusion would not have been helpful. For

the above-mentioned reasons, this small control group was excluded from final analysis.

Of the total 103 patients included in the final analysis, 53 were diagnosed with malignant disease (31 in group I and 22 in group II) and 50 (20 in group I and 30 in group II) with a benign etiology.

## Univariate Analysis

**SUV Max.** SUV max assessed the maximum intensity of uptake in the hilar regions on the PET scans (SUV max for group I patients and SUV max of first scan in group II patients). Of 103 patients, those with a diagnosis of malignancy had a significantly higher SUV max ( $6.6 \pm 4.1$ ) than did those with a benign etiology ( $3.5 \pm 1.0$ ) ( $P < 0.001$ ;  $t$  test).

**Symmetry.** Symmetry assessed the difference in SUV max between the left and right hilar regions in patients on their first scan. It was measured by the absolute difference as well as the percentage difference. When we considered the absolute value, the malignant group had a significantly higher difference ( $1.8 \pm 1.7$ ) than did the benign group ( $0.57 \pm 0.54$ ) ( $P < 0.01$ ;  $t$  test). When we considered the percentage difference, the malignant group also had a significantly higher difference ( $30.2\% \pm 22.0\%$ ) than did the benign group ( $17.1\% \pm 14.3\%$ ) ( $P < 0.01$ ;  $t$  test). Figure 1 illustrates bilateral symmetric and low hilar uptake that was ultimately proven to be a case of benign etiology. On the other hand, Figure 2 shows an example of asymmetric uptake that was revealed to be malignant on biopsy.

**Purity.** Purity was measured by the absence of  $^{18}\text{F}$ -FDG-avid mediastinal nodes in the chest outside the hilar areas (e.g., paratracheal, subcarinal, or prevascular nodes). Patients with an impure scan had at least 1 or more areas of  $^{18}\text{F}$ -FDG nodal uptake in a nonhilar region. Of the 53 patients who were diagnosed with malignant disease, compared with only 9 of 50 patients with benign disease, 42 had an impure scan. Hence, an impure scan was significantly associated with malignant disease, as 79% of patients with

**TABLE 1**  
Comparison of Parameters in 4 Groups of Patients

First scan	Patients...			
	Without cancer	With granulomatous disease	Without metastatic disease	With metastatic disease
Total	11	10	50	53
SUV max	$1.79 \pm 0.46^*$	$9.85 \pm 7.58^{*†}$	$3.48 \pm 0.91^*$	$6.61 \pm 4.12^\dagger$
Impurity number (%)	0 (0%)	7 (70%)	9 (18%)	42 (79%)
Percentage symmetry { $100\% \times  SUV_R - SUV_L  \div$ { $(SUV_L + SUV_R)/2$ }	$14.4 \pm 8.0$	$36.2 \pm 21.1^\dagger$	$17.1 \pm 14.3$	$30.8 \pm 21.8^\dagger$

\*ANOVA with Tukey post hoc test,  $P < 0.05$ , different from metastatic-disease group (average  $\pm$  SD or number of patients (%)).

$^\dagger$ ANOVA with Tukey post hoc test,  $P < 0.05$ , different from benign and no-metastatic-disease groups.

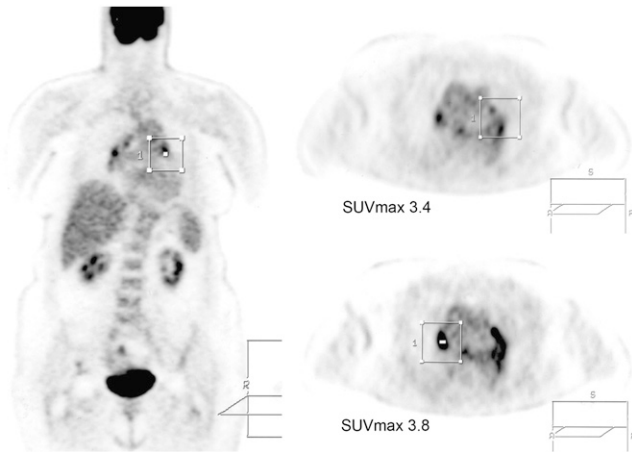


**FIGURE 1.** Benign findings: Images show foci of mild symmetric  $^{18}\text{F}$ -FDG uptake limited to hilar nodes (pure).

an impure scan, compared with 18% of patients with a pure scan ( $P < 0.001$ ;  $\chi^2$  test), had malignancy. Figure 3 illustrates malignant disease associated with uptake in mediastinal nodes outside the hilum, namely the subcarinal and the right pretracheal nodes. (Fig. 1 is an example of pure and Fig. 2 is an example of impure [right pretracheal nodes] uptake.)

*Node Size Determined by CT.* Subjective assessment of node size on CT was performed in 35 patients whose entire evaluation was done with PET/CT (21 initial staging and 14 patients with sequential PET). An enlarged node was asso-

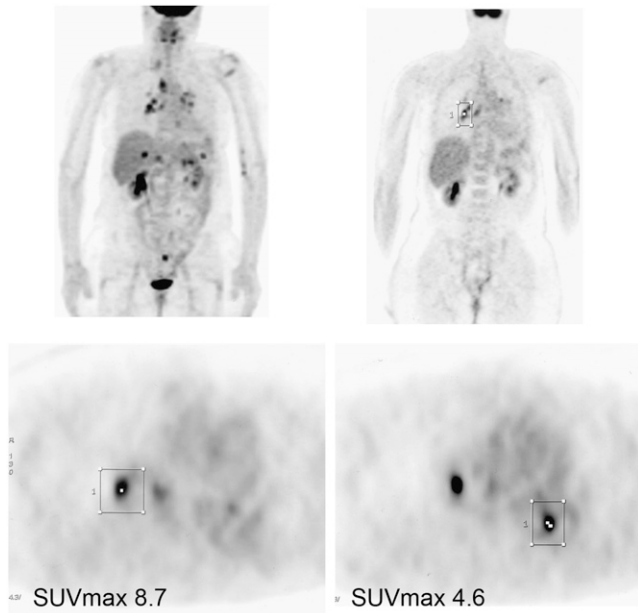


**FIGURE 2.** Malignant findings: Foci of asymmetric  $^{18}\text{F}$ -FDG uptake in hilar nodes. Note also elevated uptake in right pretracheal nodes (impure).

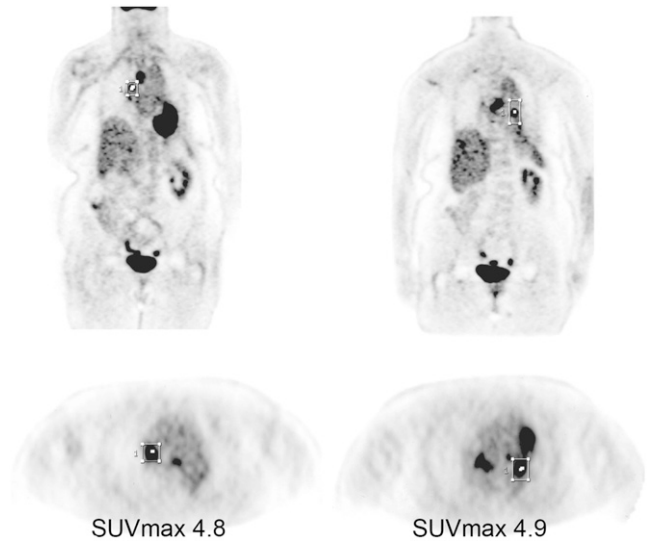


**FIGURE 3.** Malignant findings: Typical example of so-called impure uptake with involvement of right pretracheal and subcarinal nodes by  $^{18}\text{F}$ -FDG-avid process.

ciated with a high likelihood for malignancy (odds ratio, 4.77; 95% confidence interval [CI], 1.14–19.98;  $P = 0.027$ ).

*Primary Tumor.* The patients included in this study had a variety of primary malignancies: 12 patients had breast cancer, 20 had colorectal, 37 had lymphoma, and 34 had other malignancies (7 head and neck, 6 melanomas, 5 esophageal, 5 unknown primaries, 2 GIST, 2 NET, 2 testicular, 1 cholangiocarcinoma, 1 anal, 1 renal, 1 prostate, and 1 bladder cancer).  $\chi^2$  analysis of the primary cancer site and the percentage of malignant hilar foci revealed that colorectal cancer was associated with the lowest incidence of malignant hilar foci, accounting for only 25% (5/20), whereas breast cancer had 66% (8/12), lymphoma had

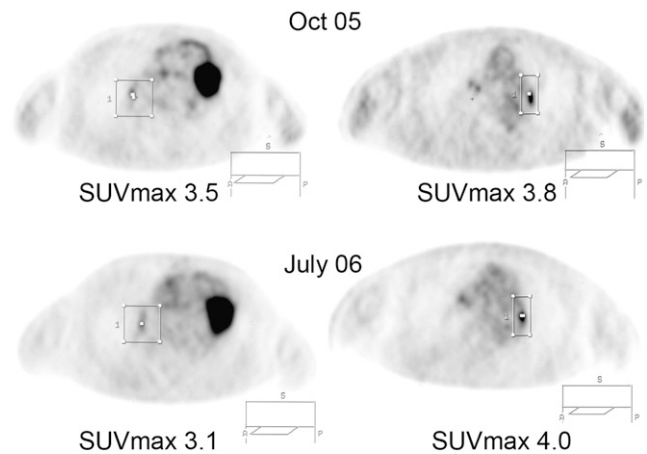


**FIGURE 4.** Benign findings: Two sequential PET studies demonstrating stable  $^{18}\text{F}$ -FDG-avid foci in hilar nodes despite intervening chemotherapy for colorectal cancer. Hilar uptake was also mild.

51% (19/37), and other had 63% (21/33) malignant hilar nodes ( $P = 0.038$ ;  $\chi^2$  test).

**Stability.** Stability of uptake was measured in the group II patients (subset of 53 patients who had at least 2 sequential PET scans) only. It assessed the difference in SUV max between the first and second scans and was measured by the absolute difference as well as the percentage difference; it did not take into account the direction of change (increase vs. decrease). When the absolute value was considered, the malignant group had significantly more change ( $2.7 \pm 2.5$ ) between the 2 scans than did the benign group ( $0.73 \pm 1.1$ ) ( $P < 0.01$ ;  $t$  test). The percentage value also demonstrated that the malignant group had more change ( $57.0\% \pm 53.0\%$ ) than did the benign group ( $19.6\% \pm 25.2\%$ ) ( $P < 0.01$ ;  $t$  test). Figure 4 shows a patient with stable mild and symmetric uptake identified as benign. Figure 5 illustrates proven metastatic mediastinal disease that was described as high symmetric uptake that decreased significantly on scan 2 after intervening treatment.

After the univariate analysis, odds ratios for malignant or benign etiology can be drawn. Significant results were found for SUV max, purity, symmetry, and, for group II patients, difference in SUV max. For instance, for every unit increase

in SUV max, the odds for malignancy increase by 1.70 (95% CI, 1.31–2.21;  $P < 0.001$ ). If the pattern of hilar uptake is pure, the odds of malignancy decrease by 0.06 (95% CI, 0.02–0.15;  $P < 0.001$ ). And for every percentage-point change in SUV max between scan 1 and scan 2, the odds for malignancy increase by 1.03 (95% CI, 1.01–1.05;  $P = 0.002$ ), suggesting that hilar uptake of benign etiology is stable over time. Change in SUV max was found to occur in both directions (increase or decrease).

All data obtained from the univariate analysis are summarized in Table 2.

### Multivariate Analysis

The following variables as potential predictors of malignancy were studied: SUV max, purity, primary site, and symmetry. Variability of uptake over time was not included because of the lack of a sufficient number of patients; enlarged size by CT could not be included for the same reason. Both the forward- and the backward-selection model building yielded SUV max and purity as significant predictors of malignancy. Other indicators did not significantly improve model fit. For SUV max, the odds of malignancy increased by 1.54 (95% CI, 1.16–2.05) for each unit increase in SUV. The odds of malignancy decreased by 0.08 (95% CI, 0.03–0.22) if hilar uptake was pure. Data are presented in Table 3.

Using our population and the results of the stepwise logistic model, the probabilities of malignancy are shown for pure and impure lesions as a function of SUV max in Figure 6.

### DISCUSSION

Abundant data on the accuracy of PET for the detection of malignant mediastinal nodes in patients with lung cancer have been reported (5–10). However, this is the first investigation, to our knowledge, to address the clinical significance of a common and puzzling finding on PET and PET/CT scans of patients with various primary cancers located outside the lungs in a systematic manner.

After an exhaustive search of the literature, 2 investigations addressing this diagnostic dilemma in a marginal manner were found. The first evaluated the performance of PET/CT for the evaluation of nodal disease in patients with esophageal cancer (11). A high rate of false-positive hilar foci was found that was mainly responsible for a relatively low specificity for PET. A second study evaluated the sensitivity and specificity of PET in lymphoma. In this study, when defining the criteria for positive PET findings,  $^{18}\text{F}$ -FDG uptake in hilar foci was not considered as indicative of lymphomatous involvement because of the known high incidence of inflammation in this location. Also, foci of symmetric nodal mediastinal uptake were not classified as positive in this study (12).

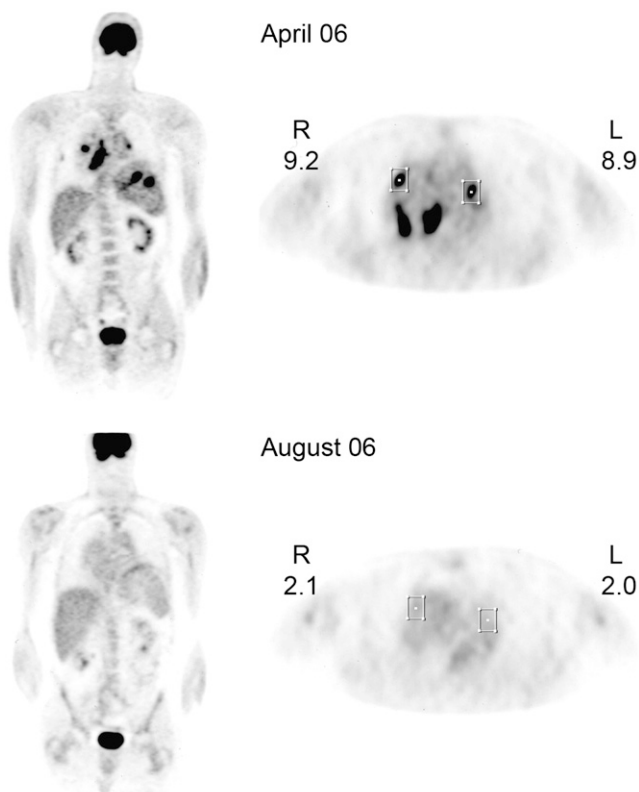


**FIGURE 5.** Malignant findings: Patient with breast cancer with significant decline in hilar uptake after treatment. Note also  $^{18}\text{F}$ -FDG-avid foci in subcarinal nodes on initial study.

**TABLE 2**  
Univariate Analysis of Variables Associated with Malignancy

Variable	n	Odds ratio	95% CI		P
			Lower	Upper	
SUV max: increase in odds of malignancy per unit SUV max	103	1.70	1.31	2.21	<0.001
Purity: reduced odds of malignancy if pure	103	0.06	0.02	0.15	<0.001
Percentage symmetry: increase in odds per unit percentage L to R difference in SUV	103	1.04	1.02	1.07	<0.001
Primary site: change in odds relative to sites other than breast, colorectal, or lymphoma					0.038
Other	34	1			
Breast	12	1.24	0.31	4.95	
Colorectal	20	0.21	0.06	0.70	
Lymphoma	37	0.65	0.25	1.68	
Percentage difference in SUV max: increase in odds per percentage change in SUV on 2 scans	52	1.03	1.01	1.05	0.002
Enlargement on CT: increase in odds of malignancy if nodes are enlarged on CT	35	4.77	1.14	19.98	0.027

SUV max, purity, primary site, enlarged size by CT, and symmetry (absolute value of left-to-right SUV difference) were tested as potential predictors of malignancy. In reduced dataset of patients with 2 scans, change in SUV max (absolute value of change in SUV max divided by initial SUV max) was also tested.

The following are 2 limitations to this study. First, the study is retrospective. Second, some variables such as SUV change on sequential PET scans and size by CT could not be included in the multivariate analysis because of the small number of patients studied (most of the patients in our study were scanned before our system was upgraded from PET to PET/CT in 2006). However, univariate analysis revealed that both variables may be important indicators. In particular, as far as CT evaluation is concerned, evidence in the literature suggests that large nodes are more likely to harbor tumor cells than are small ones when the primary tumor is in the lung (13,14). To the best of our knowledge, no studies address this issue of when the cancer is outside the lungs.

However, a study by Shiraki (15) demonstrates that false-positive findings are more often associated with enlarged nodes. Moreover, accurate quantitative and reproducible

measurement of hilar node size may be difficult in the absence of intravenous contrast. Despite this limitation, and in view of our results, adding whatever information is available from the CT component will increase reader's confidence and enhance accuracy for resolving this diagnostic dilemma.

It can be argued that the SUV measurements obtained from the PET-alone system are not comparable to those measurements obtained from the PET/CT. First, it is the same PET equipment—it has just been upgraded to PET/CT by adding a CT component. Also, the protocol for the acquisition of the PET component was identical before and after the upgrade. The only difference between the 2 systems is the attenuation-correction method. We have reviewed the literature on this method. In body areas in which no oral contrast and no metallic hardware are present, differences of 6%–8% in SUV measurement have been

**TABLE 3**  
Variables Associated with Malignancy after Multivariate Analysis

Variable	Odds ratio	Lower 95% CI	Upper 95% CI
SUV max: increase in odds of malignancy per unit elevated SUV max	1.54	1.16	2.05
Purity: reduced odds of malignancy if pure	0.08	0.03	0.22

SUV max, purity, primary site, and percentage symmetry were evaluated as potential predictors of malignancy. Both forward- and backward-selection model building yielded SUV max and purity as significant predictors of malignancy. Other indicators did not significantly improve model fit.

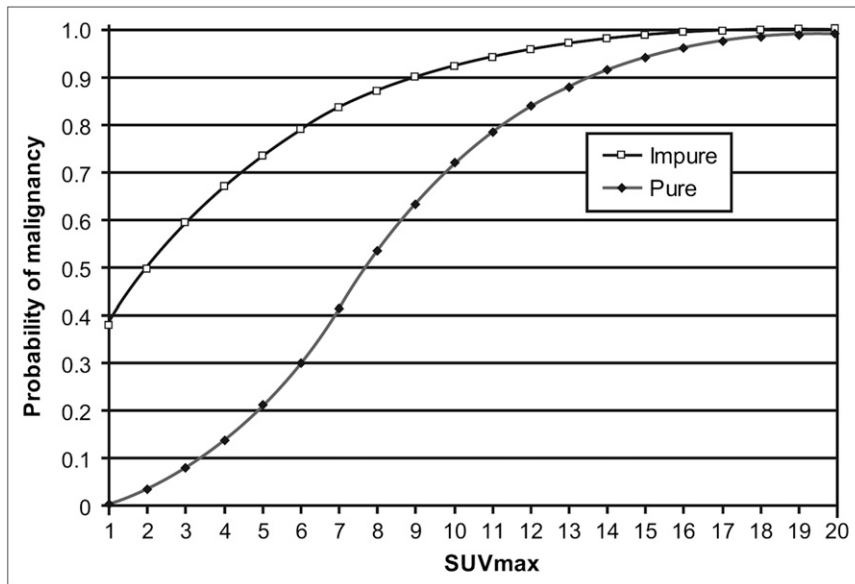


**FIGURE 6.** Theoretic probability of malignancy as it relates to SUV max in patients with pure vs. impure pattern of  $^{18}\text{F}$ -FDG hilar uptake.

reported between the 2 attenuation-correction methods (16). The same conditions apply to our study. Such a small difference would not affect hilar features such as purity or symmetry but may have a small effect on absolute SUVs and changes observed on sequential scans. In most patients, the SUV changes exceeded this range. Moreover, only 10 of 103 patients had sequential scans performed with different system configurations.

## CONCLUSION

According to the results of our study, independent features of bilateral  $^{18}\text{F}$ -FDG-avid hilar foci are associated with a benign etiology. In particular, a low level of uptake (SUV max < 3), limited to the hila, is associated with a low incidence of malignant etiology. When this low incidence is combined with low pretest likelihood, the resulting probability may be so low that it may not be necessary to recommend a follow-up PET examination or tissue diagnosis in these patients. Other variables associated with a benign outcome, which may not be independent, are symmetry and stability of uptake, despite intervening therapy, on sequential studies. Finally, a colorectal primary is associated with a significantly decreased incidence of malignant hilar nodes.

On the other hand, the presence of elevated asymmetric uptake in hilar and other mediastinal nodes that appear enlarged on CT, in the absence of signs of silicosis or anthracosis or asbestosis or without a history of sarcoidosis, should raise a degree of suspicion and may require tissue diagnosis for confirmation. Occasionally, granulomatous disease will be found.

## ACKNOWLEDGMENTS

We acknowledge Doris Eve Jensen for editorial assistance and Michael Ciarmiello for preparing the illustrations.

## REFERENCES

1. Kirschner PA. Cervical mediastinoscopy. *Chest Surg Clin N Am.* 1996;6: 1–20.
2. Rintoul RC, Skwarski KM, Murchison JT, et al. Endobronchial and endoscopic ultrasound-guided real-time fine needle aspiration for mediastinal staging. *Eur Respir J.* 2005;25:416–421.
3. Yasufuku K, Chiyo M, Sekine Y, et al. Real-time endobronchial ultrasound-guided transbronchial needle aspiration of mediastinal and hilar lymph nodes. *Chest.* 2004;126:122–128.
4. Lin J, Iannettoni MD. The role of thoracoscopy in the management of lung cancer. *Surg Oncol.* 2003;12:195–200.
5. Kim YK, Lee KS, Kim BT, et al. Mediastinal nodal staging of nonsmall cell lung cancer using integrated  $^{18}\text{F}$ -FDG PET/CT in a tuberculosis-endemic country: diagnostic efficacy in 674 patients. *Cancer.* 2007;109:1068–1077.
6. Rodríguez Fernández A, Gómez Río M, Llamas Elvira JM, et al. Diagnosis efficacy of structural (CT) and functional (FDG-PET) imaging methods in the thoracic and extrathoracic staging of non-small cell lung cancer. *Clin Transl Oncol.* 2007;9:32–39.
7. Yi CA, Lee KS, Kim BT, et al. Efficacy of helical dynamic CT versus integrated PET/CT for detection of mediastinal nodal metastasis in non-small cell lung cancer. *AJR.* 2007;188:318–325.
8. Alongi F, Ragusa P, Montemaggi P, Bona CM. Combining independent studies of diagnostic fluorodeoxyglucose positron-emission tomography and computed tomography in mediastinal lymph node staging for non-cell lung cancer. *Tumori.* 2006;92:327–333.
9. Bryant AS, Cerfolio RJ, Klemm KM, Ojha B. Maximum standard uptake value of mediastinal lymph nodes on integrated FDG-PET-CT predicts pathology in patients with non-small cell lung cancer. *Ann Thorac Surg.* 2006;82:417–422.
10. Takamochi K, Yoshida J, Murakami K, et al. Pitfalls in lymph node staging with positron emission tomography in non-small cell lung cancer patients. *Lung Cancer.* 2005;47:235–242.
11. Yoon YC, Lee KS, Shim YM, Kim BT, Kim K, Kim TS. Metastasis to regional lymph nodes in patients with esophageal squamous cell carcinoma: CT versus FDG PET for presurgical detection prospective study. *Radiology.* 2003;227:764–770.

12. Castellucci P, Zinzani P, Pourdehnad M, et al.  $^{18}\text{F}$ -FDG PET in malignant lymphoma: significance of positive findings. *Eur J Nucl Med Mol Imaging*. 2005;32:749–756.
13. Ikeda K, Nomori H, Mori T, Kobayashi H, Iwatani K, Yoshimoto K. Size of metastatic and nonmetastatic mediastinal lymph nodes in non-small cell lung cancer. *J Thorac Oncol*. 2006;1:949–952.
14. Gould M, Kuschner W, Rydzak C, et al. Test performance of positron emission tomography and computed tomography for mediastinal staging in patients with non-small-lung cancer: a meta-analysis. *Ann Intern Med*. 2003;139:879–892.
15. Shiraki N, Hara M, Ogino H. False-positive and true-negative hilar and mediastinal lymph nodes on FDG-PET: radiological-pathological correlation. *Ann Nucl Med*. 2004;18:23–28.
16. Visvikis D, Costa DC, Croasdale I, et al. CT-based attenuation correction in the calculation of semi-quantitative indices of [ $^{18}\text{F}$ ]FDG uptake in PET. *Eur J Nucl Med Mol Imaging*. 2003;30:344–353.